

PEROVSKITES BOOSTED BY METAL OXIDES AS A CATALYST FOR THE PARTIAL OXIDATION OF METHANE

SILVANA DWI NURHERDIANA*, NURUL WIDIASTUTI**, TRIYANDA GUNAWAN**, WITRI WAHYU LESTARI***, RINO RAKHMATA MUKTI****, #HAMZAH FANSURI**

*Department of Chemical Engineering, Faculty of Technology, Universitas Pembangunan Nasional "Veteran" Jawa Timur, 60294, East Java, Indonesia

**Department of Chemistry, Faculty of Science and Data Analytics, Institut Teknologi Sepuluh Nopember, 60111, East Java, Indonesia

***Department of Chemistry, Faculty of Mathematics and Natural Sciences, Sebelas Maret University, Jl. Ir. Sutami No. 36A Kentingan, Jebres, Surakarta, 57126, Indonesia

****Division of Inorganic and Physical Chemistry, Research Center for Nanoscience and Nanotechnology, Bandung Institute of Technology, Bandung, Indonesia

#E-mail: h.fansuri@chem.its.ac.id

Submitted December 18, 2021; accepted January 18, 2022

Keywords: Perovskite oxide, Metal oxide, Methane conversion, Granule catalyst, Energy research, Energy

This research aims to study the comprehensive identification of the synthesis, characterisation and performance tests of $La_{0.6}Sr_{0.4}Co_{0.2}Fe_{0.8}O_{3-\delta}$ (LSCF) and $La_{0.7}Sr_{0.3}MnO_{3-\delta}$ (LSM) granule-form catalysts with a CeO_2 and NiO addition for the POM reaction. The LSCF and LSM powder were firstly prepared using the solid-state reaction method. The granules were firstly prepared in a form of pellet, then crushed and sieved into a size of ± 1 mm. The performance study begins with a pre-treated process, by flowing 5 % O_2 gas ($30 \text{ mL}\cdot\text{min}^{-1}$) in the fixed-bed reactor at 600°C . The product was analysed using Agilent HP 6890 gas chromatography equipped with an Agilent HP 19095P-Q04 column and a FID detector. The results showed that the LSCF achieved 50.03 % methane conversion which is lower than the LSM performance of 56.41 %. The CeO_2 addition in both the LSCF and LSM revealed an increasing performance by increasing the reaction time. NiO addition resulted in a slower increase in the reaction time, which can be caused by the rate of carbon deposition formation. Based on the obtained results, the bifunctional catalyst has the potential to be developed into another module with a larger effective surface area, such as a multiple-thin layer membrane or hollow fibre membrane.

INTRODUCTION

Natural gas is an important energy source containing methane as the main component. Methane is difficult to convert into a liquid phase and it also contributes to global warming, whose impact is 21 times greater than carbon dioxide (CO_2) [1, 2]. Methane conversion into value-added chemicals, such as synthesis gas (syngas, CO and H_2), is one of many options to reduce methane emissions, which can be further converted into hydrocarbons as raw materials for the petrochemical, pharmaceutical, and polymer industries through the Fischer-Tropsch reaction [3]. However, the conversion process is quite complicated, especially in the minimisation of unwanted oxidation reactions. Syngas is an intermediate product [4] and methane has very strong and localised C-H bond with a bond energy of $413 \text{ kJ}\cdot\text{mol}^{-1}$ [5], both of which can be further oxidised to CO_2 and H_2O . Therefore, the development of methane conversion into value added materials is an important concern in catalyst research. The methane conversion can be carried out in several

ways, such as dry reforming (Equation 1), steam reforming (Equation 2), and the partial oxidation of methane (POM) (Equation 3).



Based on the above equations, the POM reaction shows several advantages, including energy savings, due to the exothermic process and the product ratio of $H_2:CO$ is 2:1, which is suitable for methanol synthesis [6]. The POM reaction generally occurs at a high temperature of around 1127°C under room pressure without employing a catalyst. Moreover, catalyst applications reached lower reaction temperatures as reported elsewhere [7]. The POM reaction requires a certain amount of oxygen in order to form syngas to hinder the excess amount of oxygen to produce a certain amount of CO and H_2 instead of CO_2 and H_2O . An oxygen vacancy lattice-based material, namely perovskite oxide, actively contributed

the controlled oxygen production which separated from the air [8].

Perovskite oxide is well-known as a mixed ionic and electronic conductor (MIEC) material which occurs from oxygen vacancies in the lattice structure [9, 10]. It has also been proven to be a catalyst for syngas production, solid oxide fuel cells (SOFCs) and other methane conversion reactions [11]. The release of oxygen ions causes oxygen vacancies in the crystal lattice and can be replenished by other oxygen ions through the re-oxidation process [12]. Perovskite has a crystal cubic structure with a general formula of ABO_3 , in which site A is usually occupied by an alkaline or alkaline group elements, such as La, Na, Ca, Sr, or Ba, while site B is filled by transition metal groups. The ionic and electronic conductivity can be increased by the modification of the metal substitution of cations at sites A and/or B with the general formula $A_{1-x}A'_xB_{1-y}B'_yO_{3-\delta}$ [13].

Perovskite oxide based on $La_{1-x}Sr_xCo_{1-y}Fe_yO_{3-\delta}$ (LSCF) has been proven to successfully deliver oxygen ions through the lattice structure instead of the pores and has the ability to separate oxygen ions from the air [14]. In addition, La-Mn-based perovskite showed good thermal stability so that it can be potentially applied in the POM reaction which generally occurs at high temperatures of around 500 - 900°C. The substitution of site A in La-Mn-based perovskites with Sr^{2+} ions increased the catalytic activity of the methane oxidation reaction [15, 16]. Based on this, LSCF and LSM have potential to be suppliers of the controlled oxygen separated from the air and as a catalyst for converting methane. However, it revealed low oxygen permeation and easily reacts with carbon dioxide (CO_2) [17, 18].

Other than that, metal oxides have shown to have good ionic conductivity, specifically cerium oxide (CeO_2) [19] and nickel oxide (NiO) [20]. CeO_2 has been reported to have good electronic conductivity which can reduce the carbon deposition and contributed as an oxygen storage material, which has a large oxygen storage capacity due to its ability to release and obtain oxygen through a redox process involving the Ce^{4+}/Ce^{3+} pairs [21]. The oxygen storage property of cerium oxide plays an important role in increasing the catalytic activity under both oxidation and reduction conditions. In addition, Ni-based catalysts have reportedly been used in methane oxidation reactions. NiO has a high oxygen transfer capacity and is usually used as a support for heat-resistant oxides to increase the thermal stability [22]. Therefore, this research aimed to study the comprehensive identification of the synthesis and characterisation of granule-based catalysts, i.e., $La_{0.6}Sr_{0.4}Co_{0.2}Fe_{0.8}O_{3-\delta}$ (LSCF) and $La_{0.7}Sr_{0.3}MnO_{3-\delta}$ (LSM) with the addition of CeO_2 and NiO. All the catalyst materials were prepared separately in a granule form, thus there is no direct particle interconnection between the perovskite and the metal oxides. The LSCF and LSM perovskite oxides were employed as the oxygen separators from the air,

while CeO_2 and NiO were used as the catalytic booster to convert the methane into value-added chemicals

EXPERIMENTAL

Materials

All the materials were received in powder form with no further purification. The LSCF and LSM perovskite oxides were self-prepared powders using the raw materials: lanthanum oxide (La_2O_3) (Merck, 99.5 %), strontium carbonate ($SrCO_3$) (Merck, 99.0 %), manganese carbonate ($MnCO_3$) (Aldrich, 99.5 %), cobalt oxide (Co_3O_4) (Merck, 99.0 %), and iron oxide (Fe_2O_3) (Merck, 99.0 %), as well as the commercially available metal oxide catalyst: nickel oxide (NiO) (Merck, 99 %) and cerium oxide (CeO_2) (Merck, 99 %). Methanol p.a. (Merck) was used as the dispersant for the perovskite preparation and 5 % O_2/N_2 gas and 10 % CH_4/N_2 gas was used for performance test.

Methodology

Perovskite Oxides (LSCF and LSM) Preparation and Characterisation

Perovskite oxide powders, namely LSCF and LSM, were synthesised by the solid state method referred to in the literature [10, 23]. In the first stage, the basic powders of both the metal oxides and carbonates were heated in an oven for 1 hour at 105 °C to remove the moisture. Next, the solid-state process begins by grinding the precursor with an appropriate mass according to the mole ratio and adding a dispersant (methanol) to increase the chance of collisions between the particles. The grinding was carried out using 15 zirconia balls and then ground using a planetary ball mill for 2 hours with a stirring speed of 600 rpm. After the milling process, the methanol is evaporated to obtain a powder mixture of the reactants. The reactant mixture was then calcined with the calcination profile step in Figure 1. The first cycle of the calcination (Figure 1a) was repeated two times, then it was ground again and the second cycle (Figure 1b) was the final stage of calcination which was carried out in one step.

The crystal phase characterisation of the perovskite oxide powder was carried out using an X-ray diffractometer. The perovskite oxide sample was placed in a diffraction cell (sample holder) then irradiated with X-rays from a Cu-K α source ($\lambda = 1.54056 \text{ \AA}$), with a current of 40 mA and an applied voltage of 40 kV. The diffraction data were taken at an angle of 2θ between 20° to 80° every 0.02 seconds. Furthermore, the diffraction pattern of the formed perovskite oxide was matched with the standard data from a PDF card (Powder Diffraction File) issued by the JCPDS (Joint Committee on Powder Diffraction Standards) in 2012.

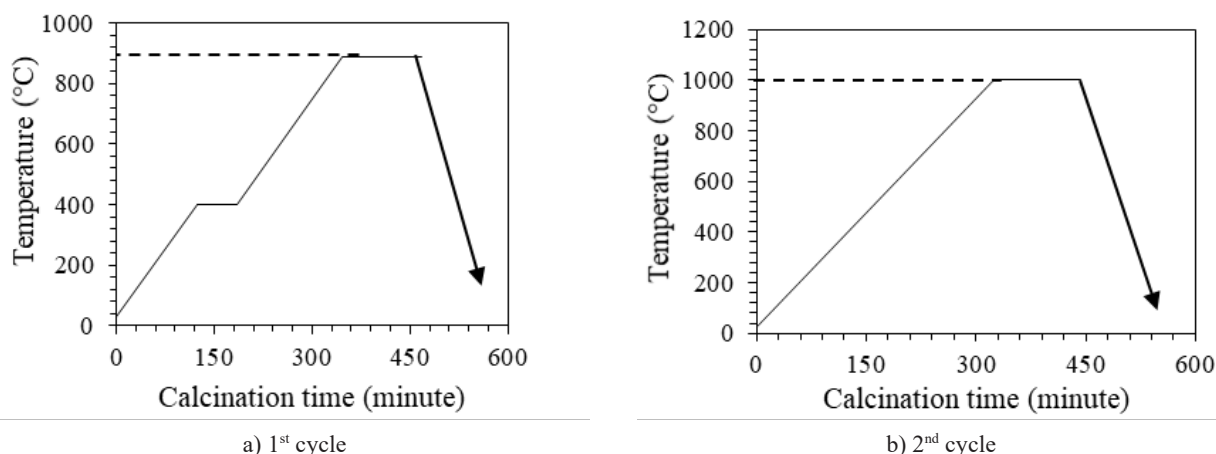


Figure 1. The calcination profile of the perovskite oxide preparation.

Fabrication of the Granule-based Bifunctional Catalyst

The obtained LSCF and LSM powder, as well as the commercial NiO and CeO₂ powders were each separately moulded into pellets (discs). As much as 0.93 g of perovskite oxide powder was put into a pellet mould with a diameter of 13 mm and then pressed with a pressure of 5-8 tonnes using a hydraulic press with holding time of 15 minutes to ensure a strong compactness. The resulting green body (pellet) was then burned through a gradual sintering process, which occurred at a temperature of 400 °C for 1 hour then continued until 890 °C for 2 hours (holding time). After the sintering process, the pellets are then crushed to form granules measuring ± 1 mm [24]. The mixture mass ratio to test the performance of the perovskite oxide and metal oxide was 9:1.

Performance Test of the Granule-based Catalyst for the Partial Oxidation of the Methane (POM) Reaction

The catalytic activity test was carried out in a fixed-bed reactor which was arranged as shown in Figure 2.

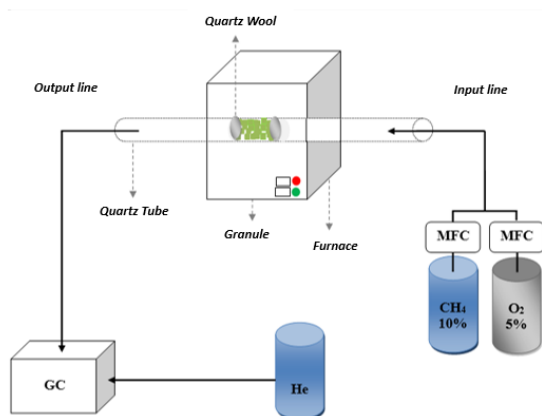


Figure 2. Illustration of the fixed-bed reactor in the POM reaction using a granule-based catalyst.

As much as 0.3 grams of the granule catalyst was put into a quartz tube flanked by quartz wool. The quartz tube was then inserted into the furnace. 5 % O₂ gas was flowed into the reactor with a flow rate of 30 mL·min⁻¹ simultaneously with the start of heating the furnace from room temperature (28 °C) to a temperature of 600 °C to ensure a successful oxidation initiation (Stage I). At 600 °C, the oxygen gas flow was stopped, then 10 % CH₄ gas was flowed at a flow rate of 30 mL·min⁻¹.

In the first hour, the product is discarded, then the gas from the reaction is accommodated in a gasbag after a reaction time of 1, 2, 3 and 5 hours (Figure 3). The resulting gas from the reaction is then accommodated into a separate gasbag. Furthermore, the product from the reaction was analysed using gas chromatography (Agilent HP 6890 series Gas Chromatography equipped with an HP 19095P-QO4 column, helium as carrier gas and a FID as the detector). The data obtained were then tabulated into a methane conversion value based on Equation 1 [20]:

$$(\text{Methane conversion in \%}) X(\%) = \frac{N_{A0} - N_A}{N_{A0}} \times 100 \%$$

where,

N_{A0} is initial methane concentration (mol)

N_A is the concentration of the detected methane in the product (mol).

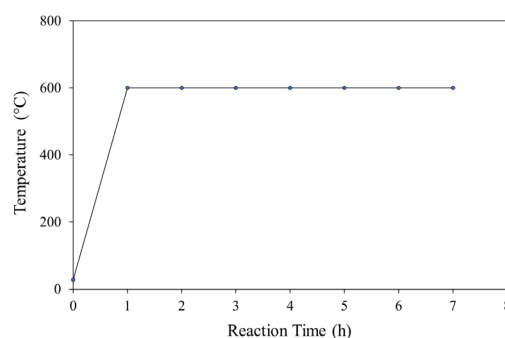


Figure 3. Temperature reaction profile of the POM reaction.

RESULTS AND DISCUSSION

Chemical Characteristics of $\text{La}_{0.6}\text{Sr}_{0.4}\text{Co}_{0.2}\text{Fe}_{0.8}\text{O}_{3-\delta}$ (LSCF) and $\text{La}_{0.7}\text{Sr}_{0.3}\text{MnO}_{3-\delta}$ (LSM) of the Pre- and Post- POM reaction

The synthesised LSCF and LSM perovskite oxide powders, both the pre- and post-POM reactions, were characterised using X-ray diffraction (XRD) at 2θ of 20° to 80° . This characterisation aims to identify the crystallinity shown in Figure 4a and 4b for the XRD pattern of LSCF and LSM, respectively. Identification of the crystallinity and the crystal structure is provided from the structure reference data $\text{La}_{0.7}\text{Sr}_{0.3}\text{Co}_{0.3}\text{Fe}_{0.7}\text{O}_{3-\delta}$ from the PDF number 01-089-1268 and LaMnO_3 from the PDF number 00-0355-1353.

The XRD results show that the perovskite oxide peaks matched, both the pre- and post-POM reactions with standard diffraction peaks. The correspondence of these peaks was shown with high intensity at the 2θ angles around 32° , 47° , and 59° as previously reported [10]. This indicates that the synthesised perovskite oxide has formed a perovskite phase in both the LSCF and LSM. Likewise with the perovskite oxide after being used for the partial oxidation reaction of methane, it still shows a perovskite phase which means there is no significant change in the structure of the perovskite oxide. Figure 4

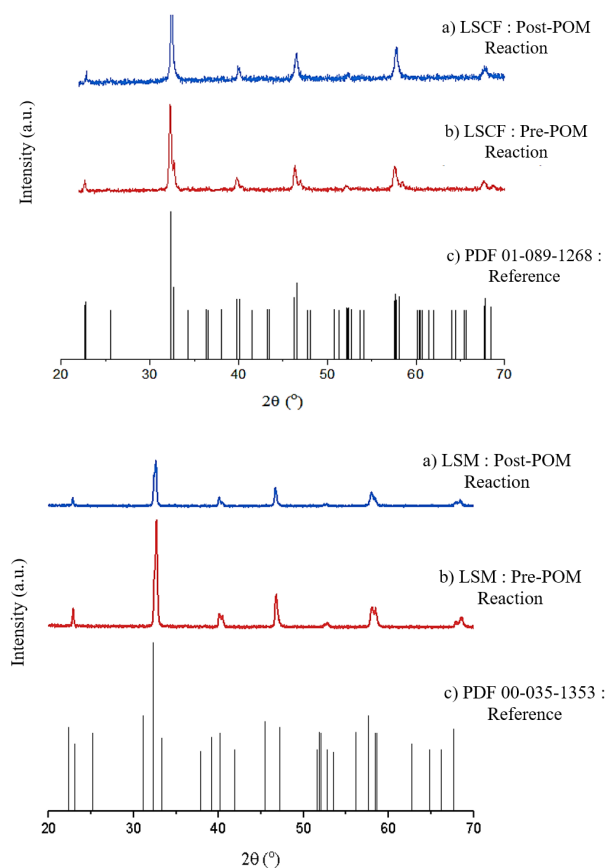


Figure 4. XRD pattern of the catalyst of the pre- and post-POM reaction.

also shows that both oxide powders have high purity with no other diffraction peaks found, such as impurities, other than the perovskite oxide peaks. However, LSM, after the reaction, showed a difference in the peak height which indicated a decrease in the crystallinity, but did not significantly change the crystal structure as evidenced by no significant peak shift as previously reported [16].

Macroscopy of Granule-based Catalyst

The synthesised catalyst used in this catalytic activity test is in the form of granules measuring ± 1 mm as shown in Figure 5 [24]. This is because the particle size of the catalyst affected the collision and catalytic activity. A too small a particle inhibited the reaction which caused an uncontrolled contact time due to the gas diffusion resistance so that the actual catalyst activity cannot be observed. If the size of the catalyst particle is too large, it can cause channelling which is known as causing no contact between the reactants and the catalyst, thereby reducing the catalytic activity. Generally, granule-based catalysts used in the fixed-bed reactors are around 1 to 20 mm in size [25].

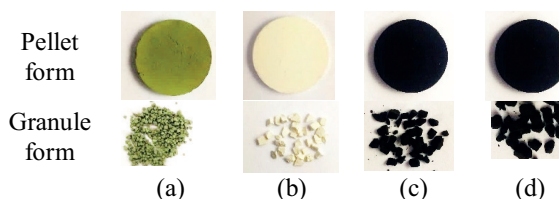


Figure 5. The apparent result of the pellet and granule-based catalyst. (a) NiO, (b) CeO_2 , (c) LSM and (d) LSCF.

Catalytic Activity of LSCF Boosted by CeO_2 and NiO

The data tabulation of the methane conversion was based on the peak area of the chromatogram and the calibration curve equation. The amount of methane that is un-oxidised/converted appears as a chromatogram peak which is represented by its area. Meanwhile, the amount of methane converted is calculated based on the difference between the initial mole and the final mole of methane as represented in Figure 6 of the LSCF- NiO and CeO_2 addition -based catalyst.

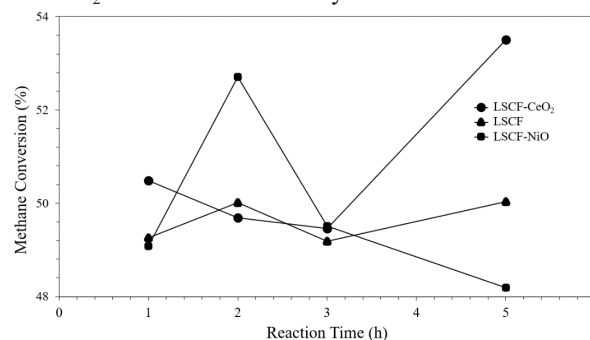
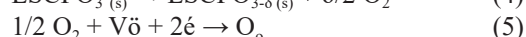
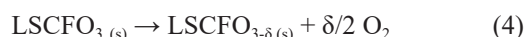
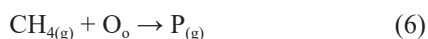


Figure 6. Methane conversion using an LSCF, LSCF- CeO_2 and LSCF-NiO-based catalyst in granule form at the reaction temperature of 600°C .

The use of the LSCF-based granule catalyst showed a stable methane conversion around 49.26 to 50.03 % to five hours of the reaction time. As mentioned in the literature, LSCF has exhibited good oxygen-conducting abilities to convert methane [25]. The mechanism of the activated LSCF can be described by Equation 4 and 5 as mentioned elsewhere, where the treatment at a temperature range of 300 – 1000 °C with oxygen flow, initiated the oxygen vacancy and formed a non-stoichiometric perovskite oxide, according to Equation 2 [26]. The non-stoichiometric degree of the oxygen is related to the oxygen vacancy, V_{O} , and the oxygen lattice, O_{O} , according to Equation 3.



The methane reduction in the LSCF-based catalyst means that the methane is oxidised by the oxygen lattice as described in Equation 6. The product, P, is then analysed using gas chromatography instruments.



Furthermore, the catalytic activity of LSCF-CeO₂ and LSCF-NiO were tested under the same reaction conditions as employed before. In this study, the results of the methane conversion as a function of time using the LSCF-CeO₂ and LSCF-NiO catalysts are shown in Figure 6. The figure shows a significant difference in the methane conversion value when employing different catalysts.

The result showed that the addition of CeO₂ to LSCF affected the catalytic activity. In the first hour after the reaction, the methane conversion was higher than that of the LSCF catalyst usage. This indicated that there was a larger conversion reaction supported in the range of the reaction time. Meanwhile, the methane conversion decreased in the second and third hours and it was possible to decrease the contact between the catalyst and the CH₄, so that the lattice oxygen interaction on the

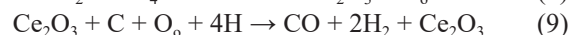
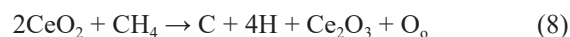
catalyst and CH₄ became less than optimal. Furthermore, there was an increase in the methane conversion at the fifth hour from 49.46 % to 53.50 % which indicated an increase in the activity of the catalyst.

CeO₂ was investigated as a suitable support for the partial oxidation of methane due to its high thermal stability, ability to store oxygen and reduce the carbon formation [27]. Apparently, there was no significant colour change in the LSCF-CeO₂ both pre- and post-POM reaction being used for the POM reaction. CeO₂ showed small change in colour and can still be used for POM reactions as presented in Figure 7. This is also supported by the increase in the methane conversion in the fifth hour of the reaction time, which automatically indicates that CeO₂ also shows a positive effect in supporting a reduction in the carbon formation [28].

The prediction mechanism showed that the CH₄ oxidation by cerium oxide is facilitated by the presence of the lattice-active oxygen on the CeO₂ surface as described in the literature [29]. This reaction involves the reduction of Ce⁴⁺ (CeO₂) to Ce³⁺ (Ce₂O₃) according to Equation 7.



The reduction of the Ce³⁺ site is related to the activation of the CH₄ to carbon as an intermediate reaction. One of the carbon reactions with lattice oxygen (carbon oxidation) can produce CO, according to the following Equations:



The addition of NiO to the perovskite oxide of LSCF 6428 affects the value of the methane conversion. In the first hour, the conversion of methane for the LSCF-NiO catalyst was 49.08 % and almost equivalent to the LSCF one, it is possible that the NiO has not yet reached a steady point so that there is not much interaction with the methane gas. In the second hour, the conversion of

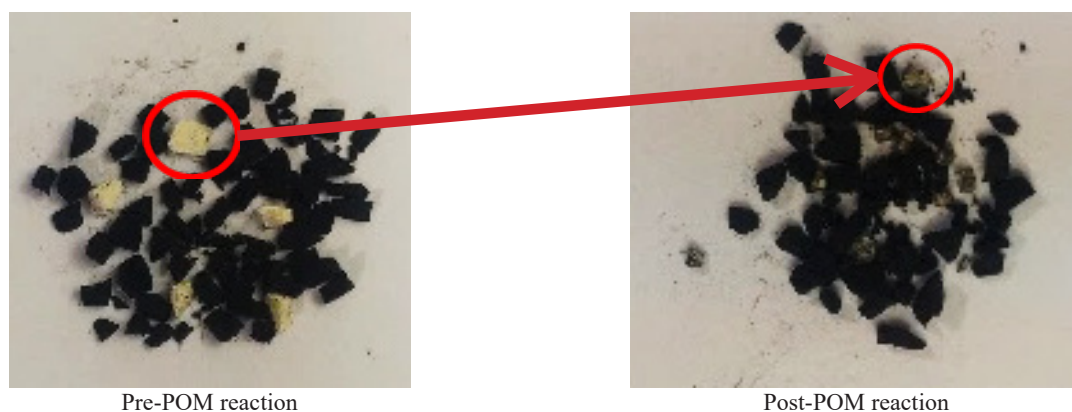
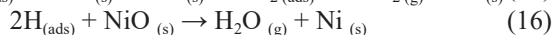
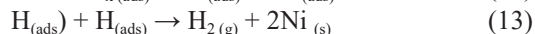
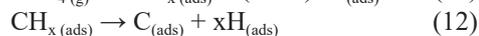
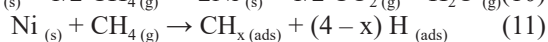


Figure 7. Image of CeO₂ addition-based catalyst from pre- to post-POM reaction.

methane increased to 52.71 % and it is very possible that this was due to the increase in the availability of oxygen in the catalyst lattice, which means that with the more available lattice oxygen, the higher the interaction with the methane. However, over time, the catalyst experienced a decrease in the methane conversion to 49.51 % and 48.19 % in the third and fifth hours, respectively. The cause of the decrease in the methane conversion can be caused by several factors, such as the formation of carbon in the catalyst, the reduction of NiO by CH₄ to Ni, and the deactivation of the Ni catalyst. The reaction involving the interaction between CH₄ and NiO [30] corresponds to the following Equations:



The performance of NiO-based catalysts decreases over time due to the large amount of carbon deposition on the catalyst [22]. In this study, there was a physical change in the colour of the NiO. Before being used for the reaction, the NiO was green and the colour after being used for the reaction is presented in Figure 8.

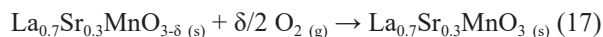
Catalytic Activity of LSM boosted by CeO₂ and NiO

The results of the methane conversion in the POM reaction when employing LSM, LSM-CeO₂ and LSM-NiO as the catalyst are shown in Figure 9. The LSM employed catalyst produced methane conversion at 1, 2, 3 and 5 hours of reaction time of 52.11, 51.11, 51.94 and 56.41 %, respectively. From the results of the methane conversion, it can be seen that after 1 hour of reaction time, 52.11 % of the methane was converted, but after 2 hours of reaction, there was a 1 % decrease in the

methane conversion to 51.11 %. After 3 hours of reaction time, the methane conversion increased from 0.93 % to 51.94 %. After 5 hours of reaction time, the converted methane was 56.41 %, where there was an increase of 4.47 %.

The increase in the methane conversion could be due to the reactions still going on and the lattice oxygen that was still present in the perovskite structure of the LSM as indicated by the XRD analysis of the LSM of the post-POM reaction for 5 hours as shown in Figure 9. After 5 hours of reaction time, LSM is still present in the perovskite phase, so there is still lattice oxygen available that can react with the methane. However, after being used for 5 hours in the reaction, the crystallinity of the LSM decreased markedly with a reduced intensity as seen from the diffractogram.

The catalytic activity of LSM can be determined based on the methane conversion value in the POM reaction at a temperature of 600 °C. Prior to the reaction, the LSM was oxidised with 5 % oxygen at a flow rate of 30 mL·min⁻¹ during the heating of the catalyst, starting from room temperature (28 °C) until a temperature of 600 °C was reached. The purpose of flowing oxygen is so that the oxygen vacancy in the LSM is filled with oxygen as shown in Equation 17.



The methane reaction with oxygen derived from the oxygen lattice of perovskite, the prediction mechanism for the partial oxidation of methane as shown in Equation 18 and 19 which refers to the method in Nalbadian et al [31].

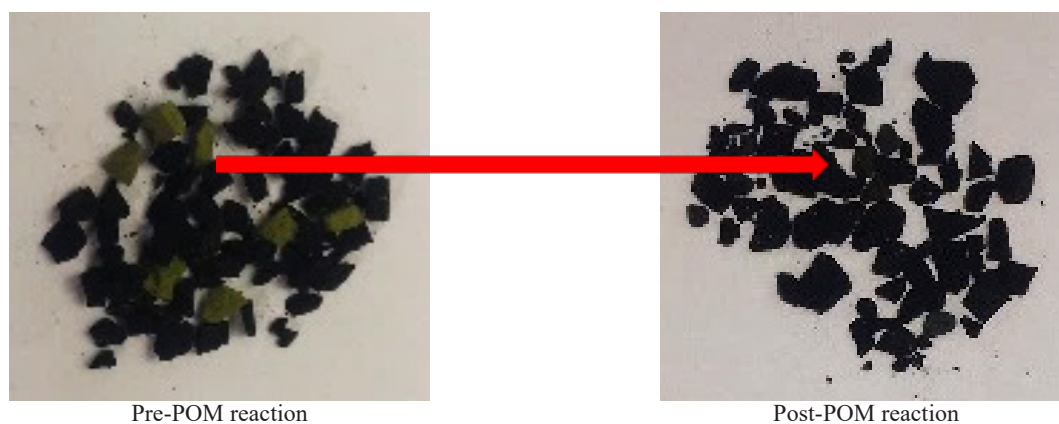
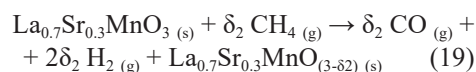
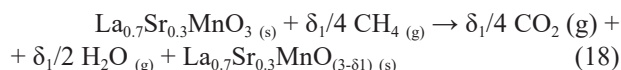


Figure 8. Image of the NiO addition-based catalyst from the pre- to post-POM reaction.

At a reaction temperature of 600 - 900 °C, the lattice oxygen in the perovskite is less reactive, but more selective towards the formation of CO and H₂ [8], so that the formation of other products, such as CO₂ and H₂O, can be minimised. The POM reaction occurs between methane and lattice oxygen by the LSM. Methane is adsorbed on the perovskite surface and interacts with the lattice oxygen to react and form products (CO and H₂). When the product desorption occurs and is separated from the perovskite structure, the amount of oxygen will decrease and the Mn metal in the perovskite will be reduced from Mn⁴⁺ to Mn²⁺ so that the perovskite structure remains stable, so that the perovskite is in a reduced state [32].

The results of the methane conversion by using LSM-CeO₂ as the catalyst at 1, 2, 3 and 5 hours were 50.36, 50.46, 53.44 and 53.74 %, respectively, as shown in Figure 9. It can be seen that in the reaction time of 3 hours achieved up to 53.44 %, slightly higher than the methane conversion with the LSM catalyst which is 51.94 % due to the influence of the CeO₂. However, at the POM reaction time of 5 hours, the methane conversion with the LSM-CeO₂ catalyst was lower than the methane conversion value with the LSM catalyst. The low methane conversion value can be caused by the CeO₂ being less active as a catalyst at a reaction temperature of 600 °C which, due to the interaction between methane and CeO₂ catalyst, is very low. CeO₂ compounds can play an active role as a catalyst for POM reactions at reaction temperatures > 650 °C [33].

The results of the methane conversion when using LSM-NiO as the catalyst at the reaction times of 1, 2, 3 to 5 hours are 61.37, 61.15, 60.97 and 58.12 %, respectively, as shown in Figure 9. The methane conversion value in the POM reaction with the LSM-NiO catalyst has a greater value than the methane conversion value in the use of the LSM catalyst alone for the entire observed reaction time. This shows that the addition of the NiO catalyst to LSM 73 has an effect on increasing the methane conversion in the POM reaction

with a temperature of 600 °C at the reaction times of 1, 2, 3 and 5 hours. The methane conversion in the POM reaction with the LSM-NiO catalyst is greater because, apart from the interaction between LSM and CH₄, there is also a good collaboration reaction between NiO and CH₄. At 5 hours, the methane conversion value in the reaction with the LSM-NiO catalyst was 58.12 % and close to the methane conversion value with the LSM catalyst, which was 56.41 %. So, it is possible that the decrease in the methane conversion occurs due to the reduced performance of the NiO catalyst in the POM reaction the longer the reaction takes place and higher formation carbon deposition occurs.

CONCLUSION

Based on the research that has been undertaken, it can be concluded that the addition of CeO₂ and NiO affects the catalytic activity of LSCF and LSM. The results of the partial oxidation of methane at 600 °C showed that the LSCF perovskite oxide was able to convert 49.26 to 50.03 % of the methane. The addition of CeO₂ to the LSCF achieved an increase in the methane conversion up to 53.50 %, while the addition of NiO to the LSCF reduced the performance. The catalytic activity of the LSM resulted in a greater methane conversion than the LSCF, namely 51.11 - 56.41 % for 5 hours of reaction time. The addition of CeO₂ into the LSM increased the methane conversion value at the third hour of the reaction time, while at the first, second and fifth hours it tends to be constant. The addition of NiO to the LSM had an effect on increasing the methane conversion value, which ranged from 58.12 - 61.37 %. However, the methane conversion tends decrease, which can be a product of the rapid formation of the carbon deposition. Therefore, the addition of metal oxides in perovskite oxide reactions have the potential to be developed, such as in the form of membranes, to increase the active surface area and avoid the accumulation of residual carbon.

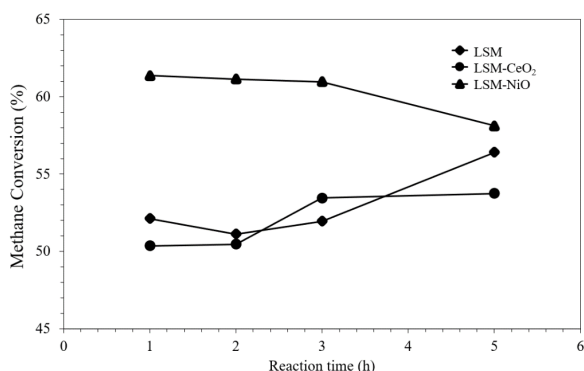


Figure 9. Methane Conversion using LSM, LSM-CeO₂ and LSM-NiO-based Catalyst in Granule Form at Reaction Temperature of 600 °C.

Acknowledgements

The authors would like to greatly thank to Directorate of Research and Community Services ITS (DRPM) Institut Teknologi Sepuluh Nopember (ITS) for the publication processing fee support through the programme of Insentif Penulisan Karya Ilmiah and funding through Program Penelitian Kolaborasi Indonesia (PPKI). The author is also grateful to Hafshah Mahfuzhoh and Fitri Nur Ariyanti, who helped carry out the research.

REFERENCES

- Fiore A. M., Jacob D. J., Field B. D., Streets D. G., Fernandes S. D., Jang C. (2002): Linking ozone pollution and climate change: The case for controlling methane. *Geophysical Research Letters*, 29(19), 25-1-25-4. doi: 10.1029/2002GL015601
- Fakayode S. O., Mitchell B. S., Pollard D. A. (2014): Determination of boiling point of petrochemicals by gas chromatography-mass spectrometry and multivariate regression analysis of structural activity relationship. *Talanta*, 126, 151–156. doi: 10.1016/j.talanta.2014.03.037
- Park M. B., Park E. D., Ahn W. S. (2019): Recent progress in direct conversion of methane to methanol over copper-exchanged zeolites. *Frontiers in Chemistry*, 7(July), 1–7. doi: 10.3389/fchem.2019.00514
- Zhu T., Flytzani-Stephanopoulos M. (2001): Catalytic partial oxidation of methane to synthesis gas over Ni-CeO₂. *Applied Catalysis A: General*, 208(1–2), 403–417. doi: 10.1016/S0926-860X(00)00728-6
- Enger B. C., Lødeng R. L., Holmen A. (2009): Modified cobalt catalysts in the partial oxidation of methane at moderate temperatures. *Journal of Catalysis*, 262(2), 188–198. doi: 10.1016/j.jcat.2008.12.014
- Al-Sayari S. A. (2013): Recent developments in the partial oxidation of methane to syngas. *Open Catalysis Journal*, 6(1), 17–28. doi: 10.2174/1876214X20130729001
- Tang P., Zhu Q., Wu Z., Ma D. (2014): Methane activation: The past and future. *Energy and Environmental Science*, 7(8), 2580–2591. doi: 10.1039/c4ee00604f
- Wei H. J., Cao Y., Ji W. J., Au C. T. (2008): Lattice oxygen of La_{1-x}Sr_xMO₃ (M = Mn, Ni) and LaMnO₃-a perovskite oxides for the partial oxidation of methane to synthesis gas. *Catalysis Communications*, 9(15), 2509–2514. doi: 10.1016/j.catcom.2008.06.019
- Niedrig C., Wagner S. F., Menesklou W., Baumann S., Ivers-Tiffée E. (2015): Oxygen equilibration kinetics of mixed-conducting perovskites BSCF, LSCF, and PSCF at 900 °C determined by electrical conductivity relaxation. *Solid State Ionics*, 283, 30–37. doi: 10.1016/j.ssi.2015.11.004
- Nurherdiana S. D., Sholichah N., Iqbal R. M., Sahasrikirana M. S., Utomo W. P., Akhlus S., Fansuri H. (2017): Preparation of La_{0.7}Sr_{0.3}Co_{0.2}Fe_{0.8}O_{3-δ} (LSCF 7328) by combination of Mechanochemical and Solid State Reaction. *Key Engineering Materials*, 744(3), 399–403. doi: 10.4028/www.scientific.net/KEM.744.399
- Gan L., Zhong Q., Zhao X., Song Y., Bu Y. (2016): Structural and electrochemical properties of B-site Mg-doped La_{0.7}Sr_{0.3}MnO_{3-δ} perovskite cathodes for intermediate temperature solid oxide fuel cells. *Journal of Alloys and Compounds*, 655, 99–105. doi: 10.1016/j.jallcom.2015.09.136
- Kang B. K., Lee H. C., Heo Y. W., Kim J. J., Kim J. Y., Lee J. H. (2013): Thermal expansion behavior of La-doped (Ba_{0.5}Sr_{0.5}Co_{0.8}Fe_{0.2})O_{3-δ} cathode material. *Ceramics International*, 39(7), 8267–8271. doi: 10.1016/j.ceramint.2013.04.012
- Sunarso J., Baumann S., Serra J. M., Meulenberg W. A., Liu S., Lin Y. S., Diniz J. C. (2008): Mixed ionic – electronic conducting (MIEC) ceramic-based membranes for oxygen separation. *Journal of Membrane Science*, 320, 13–41. doi: 10.1016/j.memsci.2008.03.074
- Sunarso J., Hashim S. S., Zhu N., Zhou W. (2017): Perovskite oxides applications in high temperature oxygen separation, solid oxide fuel cell and membrane reactor: A review. *Progress in Energy and Combustion Science*, 61, 57–77. doi: 10.1016/j.peccs.2017.03.003
- Jiang S. P. (2002): A comparison of O₂ reduction reactions on porous (La,Sr)MnO₃ and (La,Sr)(Co,Fe)O₃ electrodes. *Solid State Ionics*, 146, 1–22. doi: 10.1016/S0167-2738(01)00997-3
- Sartori F., Silva D., Ofilo T., De Souza M. (2017): Novel materials for solid oxide fuel cell technologies: A literature review. *International Journal of Hydrogen Energy*, 42(41), 26020–26036. doi: 10.1016/j.ijhydene.2017.08.105
- Athayde D. D., Souza D. F., Silva A. M. A., Vasconcelos D., Nunes E. H. M., Diniz da Costa J. C., Vasconcelos W. L. (2015): Review of perovskite ceramic synthesis and membrane preparation methods. *Ceramics International*, 42(6), 6555–6571. doi: 10.1016/j.ceramint.2016.01.130
- Ilham A. M., Khoiroh N., Jovita S., Iqbal R. M., Harmelia L., Nurherdiana S. D., et al. (2018): Morphological and Physical Study of La_{0.7}Sr_{0.3}Co_{0.2}Fe_{0.8}O_{3-δ} (LSCF 7328) Flat Membranes Modified by Polyethylene Glycol (PEG). *Journal of Applied Membrane Science & Technology*, 22(2), 119–130. doi: 10.11113/amst.v22n2.131
- Zhu X., Li Q., Cong Y., Yang W. (2008): Syngas generation in a membrane reactor with a highly stable ceramic composite membrane. *Catalysis Communications*, 10(3), 309–312. doi: 10.1016/j.catcom.2008.09.014
- Sandoval M. V., Matta A., Matencio T., Domingues R. Z., Ludwig G. A., De Angelis Korb M., et al. (2014): Barium-modified NiO-YSZ/NiO-GDC cermet as new anode material for solid oxide fuel cells (SOFC). *Solid State Ionics*, 261, 36–44. doi: 10.1016/j.ssi.2014.04.014
- Zheng Y., Li K., Wang H., Tian D., Wang Y., Zhu X., Luo Y. (2017): Designed oxygen carriers from macroporous LaFeO₃ supported CeO₂ for chemical-looping reforming of methane. *Applied Catalysis B: Environmental*, 202, 51–63. doi: 10.1016/j.apcatb.2016.08.024
- Oemar U., Hidayat K., Kawi S. (2011): Role of catalyst support over PdO-NiO catalysts on catalyst activity and stability for oxy-CO₂ reforming of methane. *Applied Catalysis A: General*, 402(1–2), 176–187. doi: 10.1016/j.apcata.2011.06.002
- Iqbal R. M., Nurherdiana S. D., Sahasrikirana M.S., Harmelia L., Utomo W.P., Setyaningsih E.P., Fansuri H. (2018). The Compatibility of NiO, CeO₂ and NiO-CeO₂ as Coating on La_{0.6}Sr_{0.4}Co_{0.2}Fe_{0.8}O_{3-δ}, La_{0.7}Sr_{0.3}Co_{0.2}Fe_{0.8}O_{3-δ} and La_{0.7}Sr_{0.3}Mn_{0.3}O_{3-δ} Ceramic Membranes and Their Mechanical Properties The Compatibility of NiO, CeO₂ and NiO-CeO₂ as a Coating. In: *IOP Conference Series: Materials Science and Engineering* (Vol. 367, p. 012032). doi: 10.1088/1757-899X/367/1/012032
- Otsuka K., Jinno K., Morikawa A. (1986): Active and selective catalysts for the synthesis of C₂H₄ and C₂H₆ via oxidative coupling of methane. *Journal of Catalysis*, 100(2), 353–359. doi: 10.1016/0021-9517(86)90102-8
- Montgolkachit C., Wanakitti S. (2008): Characterization of (La,Sr)(Co,Fe)O_{3-δ} Ferrite-Based Cathodes for Intermediate-Temperature SOFCs.pdf. *Journal of Metals, Materials and Minerals*, 18(2), 33–36.
- Scott S. P., Mantzavinos D., Hartley A., Sahibzada M., Metcalfe I. S. (2002): Reactivity of LSCF perovskites. *Solid State Ionics*, 152–153, 777–781. doi: 10.1016/S0167-2738(02)00327-2

27. Pantaleo G., Parola V. La, Deganello F., Singha R. K., Bal R., Venezia A. M. (2016): Ni/CeO₂ catalysts for methane partial oxidation: Synthesis driven structural and catalytic effects. *Applied Catalysis B: Environmental*, 189, 233–241. doi: 10.1016/j.apcatb.2016.02.064
28. Singha R. K., Shukla A., Yadav A., Sivakumar Konathala L. N., Bal, R. (2017): Effect of metal-support interaction on activity and stability of Ni-CeO₂ catalyst for partial oxidation of methane. *Applied Catalysis B: Environmental*, 202, 473–488. doi: 10.1016/j.apcatb.2016.09.060
29. Vita A. (2020): Catalytic Applications of CeO₂ -Based Materials, *Catalyst*, 10 (5), 576, 5–8. doi: 10.3390/catal10050576
30. Au C. T., Hu Y. H., Wan H. I. (1994): Pulse studies of CH₄ interaction with NiO/Al₂O₃ catalysts. *Catalysis Letters*, 27, 199–206. doi: 10.1007/BF00806993
31. Nalbandian L., Evdou A., Zaspalis V. (2011): La_{1-x}Sr_xM_yFe_{1-y}O_{3-δ} perovskites as oxygen-carrier materials for chemical-looping reforming. *International Journal of Hydrogen Energy*, 36(11), 6657–6670. doi: 10.1016/j.ijhydene.2011.02.146
32. Grundy A. N., Hallstedt B., Gauckler L. J. (2004): Assessment of the La-Sr-Mn-O system. *Calphad: Computer Coupling of Phase Diagrams and Thermochemistry*, 28(2), 191–201. doi: 10.1016/j.calphad.2004.07.001
33. Otsuka K., Wang Y., Nakamura M. (1999): Direct conversion of methane to synthesis gas through gas-solid reaction using CeO₂-ZrO₂ solid solution at moderate temperature. *Applied Catalysis A: General*, 183(2), 317–324. doi: 10.1016/S0926-860X(99)00070-8